Journal of Applied Polymer Science

Green esterification: A new approach to improve thermal and mechanical properties of poly(lactic acid) composites reinforced by cellulose nanocrystals

Jamileh Shojaeiarani,[1] **Dilpreet S. Bajwa**,[1] **Nicole M. Stark**[2]
[1]Department of Mechanical Engineering, North Dakota State University, Fargo North Dakota 58102
[2]Forest Products Laboratory, U.S. Forest Service, Madison Wisconsin 53726-2398
Correspondence to: J. Shojaeiarani (E-mail: jamileh.shojaeiarani@ndsu.edu)

ABSTRACT: Cellulose nanocrystal (CNCs)-reinforced poly(lactic acid) (PLA) nanocomposites were prepared using twin screw extrusion followed by injection molding. Masterbatch approach was used to achieve more efficient dispersion of CNCs in PLA matrix. Modified CNCs (b-CNCs) were prepared using benzoic acid as a nontoxic material through a green esterification method in a solvent-free technique. Transmission electron microscopy images did not exhibit significant differences in the structure of b-CNCs as compared with unmodified CNCs. However, a reduction of 6.6–15.5% in the aspect ratio of b-CNCs was observed. The fracture surface of PLA-b-CNCs nanocomposites exhibited rough and irregular pattern which confirmed the need of more energy for fracture. Pristine CNCs showed a decrease in the thermal stability of nanocomposites, however, b-CNCs nanocomposites exhibited higher thermal stability than pure PLA. The average storage modulus was improved by 38 and 48% by addition of CNCs and b-CNCs in PLA, respectively. The incorporation of b-CNCs increased Young's modulus, ultimate tensile stress, elongation at break, and impact strength by 27.02, 10.90, 4.20, and 32.77%, respectively, however, CNCs nanocomposites exhibited a slight decrease in ultimate strength and elongation at break. © 2018 Wiley Periodicals, Inc. J. Appl. Polym. Sci. **2018**, *135*, 46468.

KEYWORDS: biopolymer; cellulose; microscopy; mechanical properties; thermal properties

Received 4 December 2017; accepted 12 March 2018
DOI: 10.1002/app.46468

INTRODUCTION

Poly(lactic acid) (PLA) is one of the most promising biodegradable polymers and is currently produced on a large industrial scale (over 140,000 tons per year).[1–4] PLA has become an attractive sustainable alternative to petroleum-based plastics due to its processability, relatively high strength, UV stability, and low toxicity.[5,6] However, slow crystallization, low thermal resistance, and excessive brittleness limit PLA potential applications.[7–9] Improving the performance characteristics of PLA by incorporating cellulose nanocrystals (CNCs) is the subject of considerable attention, due to CNCs' nanoscale dimensions, widespread availability, superior mechanical, and thermal properties.[10,11] CNCs with high crystalline structure, high aspect ratio, and large surface area are considered as one of the ideal reinforcing agents for polymer matrices in nanocomposite industry.[12,13]

Generally, the incorporation of CNCs into the polymeric matrix through a homogeneous dispersion results in the formation of a network of matrix-CNCs with an enormous amount of interfacial contacts between polymeric matrix and CNCs owing to large surface area of CNCs.[14] The strong interfacial adhesion between nanocomposite components leads to an effective stress transfer from matrix to CNCs and consequently strengthens the resulting nanocomposites.[15] Specifically, the optimal improvement in performance characteristics of PLA-CNCs nanocomposites can be achieved through the uniform dispersion of CNCs in PLA matrix.[16,17] Therefore, CNCs dispersion and their corresponding interaction with the polymer matrix are critical factors for reinforcement purposes. However, the strong hydrophilicity of the CNCs and the presence of abundant hydroxyl groups on the surface of CNCs inhibit the homogeneous dispersion of CNCs in the most hydrophobic polymeric matrices such as PLA.[18] The formation of CNCs aggregates results in a poor dispersion in PLA matrix and impedes the improvements in the mechanical performance of the nanocomposites.[19,20]

To overcome the major problem of non-uniform dispersion of CNCs in hydrophobic PLA matrix, many chemical and mechanical approaches have been extensively studied. Most of the works have focused on improving interfacial interactions

© 2018 Wiley Periodicals, Inc.

between CNCs and PLA matrix using chemical-oriented surface modification methods. In a sialylation technique introduced by Gousse *et al.* alkylchlorosilanes was applied onto the surface of cellulose whisker as silylating agents. The modification technique required 16 h of vigorous stirring at room temperature. The results showed a good dispersion of modified cellulose whisker in solvents of low polarity (not lower than 2.37).[21] Yuan *et al.* introduced alkyenyl succinic anhydride aqueous emulsion onto the surface of cellulose whiskers to improve their solubility in different solvents. The process involved freeze drying of the suspension and then heating to 105 °C for different times (5–240 min). They reported good dispersion of modified cellulose whisker in solvent of low polarity such as 1,4-dioxane.[22] Acetate and lactate modification of CNCs was performed by dual acid application (organic acid and HCl), in which acid hydrolysis and Fischer Esterification occurred in tandem. The suspension was maintained at 150 °C in a convention oven for 3 h and then the resulting CNC slurries were freeze-dried overnight and then dried for at least 12 h to produce nanofiller powder.[23]

In another work which has been performed by Yoo *et al.* two esterification routes were used to prepare fatty acid and PLA-grafted CNCs through adding DL-lactic acid syrup and zinc acetate dehydrate catalyst. The final product was dried in this study at 50 °C for 24 h in a vacuum oven. It was claimed that the simplicity and ecofriendly aspects of their method can meet the industrial demand for scaling up the surface modification method.[24]

In most of the chemical surface modification techniques, hazardous, and toxic solvents and reactants are used to alter the hydrophilicity character of the CNCs. In addition, a small number of studies have reported some improvement in the CNCs dispersion through the polymeric matrix using different manufacturing process.[25–27]

In the current study, the influence of incorporating pristine and modified CNCs on thermal and mechanical properties of the PLA-based nanocomposite was evaluated. Modified CNCs were prepared by introducing benzoic acid as grafting agent and solvent media onto the surface of CNCs. Benzoic acid with a broad application in food industry as a nontoxic and recyclable substance, was applied onto the surface of CNCs through a solvent-free and catalyzer free technique not only to integrate the green chemistry and diminishing the environmental footprint of the chemicals but also for improving the economic feasibility.[28] Dispersion–centrifugation process was performed to remove the untreated benzoic acid from the mixture with an excess of ethanol. Modified CNCs were then solvent exchanged in a stepwise manner from ethanol to chloroform without drying in order to decrease the aggregation of CNCs. A masterbatch approach was considered to ensure the uniform dispersion of CNCs in PLA matrix. The nanocomposites were manufactured using high shear co-rotating twin screw extrusion followed by injection molding. The structure of b-CNCs and the morphology of the fractured surface of the nanocomposites were studied using electron microscopes. The effects of CNCs and b-CNCs and their concentration on mechanical, thermomechanical, and thermal properties of nanocomposites were examined.

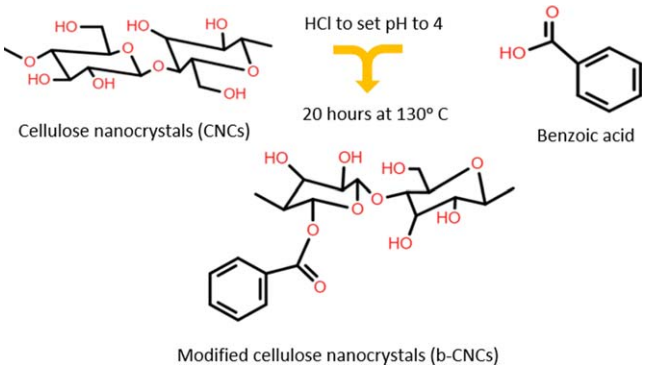

Figure 1. Esterification process to form modified CNCs (b-CNCs). [Color figure can be viewed at wileyonlinelibrary.com]

EXPERIMENTAL

Materials

PLA (2002D, $M_n = 98{,}000$ g mol^{-1}) was supplied by NatureWorks LLC (Minnetonka, MN). The specific gravity (SG) was 1.24, and the melting point (T_m) was 210 °C. Benzoic acid at 99.5% (p.a. quality) was purchased from Sigma-Aldrich (St. Louis, MO). CNCs (dimensions of 150 nm length and 7 nm width) were obtained from USDA-Forest Service (Forest Products Lab., Madison, WI). CNCs were extracted from wood-based cellulose by sulfuric acid hydrolysis. Analytical grade ethanol manufactured by Sigma-Aldrich (St. Louis, MO) was used in the experiments.

Surface Modification of Cellulose Nanocrystals

Modified CNCs (b-CNCs) were obtained through a green surface modification method using an acid ester of benzoic acid (BA) in a ratio of 1/10 (CNCs/BA) (Figure 1). In this method, benzoic acid was used as grafting agent on the surface of CNCs and solvent media above its melting point. CNCs suspension in water (10%, wt %) was sonicated for 5 min and the pH was fixed to 4 by applying hydrochloride acid (HCl, 0.1 mol L^{-1}). Benzoic acid pellets were added to the aqueous suspension of CNCs and the suspension was stirred vigorously at 130 °C for 20 h. Dispersion–centrifugation process was then repeated for six cycles to remove the untreated benzoic acid from the mixture (10,000 rpm) with a large excess of ethanol.[28] Modified CNCs were then solvent exchanged in a stepwise manner from ethanol to chloroform, a liquid medium without drying (to avoid aggregation) for the further application.

Preparation of Nanocomposites

In this work, masterbatch films with 15 wt % of cellulose nanocrystals (CNCs and b-CNCs) and 85 wt % of PLA were prepared using solvent casting method and chloroform as the solvent. PLA pellets were dissolved in chloroform under vigorous stirring at room temperature (~25 °C) for 12 h. Cellulose nanocrystals (CNCs and b-CNCs) were added to chloroform separately and to improve the dispersion of cellulose nanocrystals in chloroform, the suspension was exposed to homogenizer (IKA T50 Ultra-Turrax, Wilmington, NC) for 6 min and sonication (Misonix

Table I. Compositions of the Nanocomposite Materials

Material designation	Composition		
	PLA (wt %)	CNCs (wt %)	b-CNCs (wt %)
PLA	100	—	—
PLA-1CNCs	99	1	—
PLA-3CNCs	97	3	—
PLA-5CNCs	95	5	—
PLA-1b-CNCs	99	—	1
PLA-3b-CNCs	97	—	3
PLA-5b-CNCs	95	—	5

sonicator, Vernon Hills, IL) for 5 min in an ice bath. The cellulose nanocrystals solution was then added to PLA solution, stirred for 5 h, and was cast onto the Petri dishes and put to dry at ambient temperature for approximately 30 h.

The dried masterbatch films with 15 wt % CNCs or b-CNCs were chopped using a paper cutter (ACCO, Columbus, WI) with the approximate size of 4 by 4 mm and then diluted to nanocomposite extruded pellets with 1, 3, and 5 wt % of cellulose nanocrystals through the melt extrusion process. The chopped master batch and PLA polymer were fed into co-rotating twin screw extruder (Krauss-Maffei Co., Florence, KY) fitted with high shear elements. The barrel temperature for eight zones of extruder was set at 157, 157, 165, 162, 162, 162, 160, 160 °C (feed throat to die end), respectively, and the screw speed was set at 170 rpm. The extruded pellets were placed in an oven (Binder ED, Binder Inc., Bohemia, NY) set at 60 °C for 24 h prior to injection molding process (Technoplas Inc. SIM-5080). The final composition and codification of the samples obtained from injection molding are shown in Table I.

Characterization and Measurement

Morphology and Dimensions. The morphology and aspect ratio of CNCs and b-CNCs were investigated using a transmission electron microscopy (TEM) (JEOL Inc., Peabody, MA) operating at 2 kV. The CNCs and b-CNCs suspensions were deposited using an aqueous dispersion on a carbon-coated copper (300-mesh) TEM grids. The samples were subsequently stained to enhance the microscopic resolution.

Fractured Surface Morphology. The morphology of impact fractured surface of the nanocomposites was observed using scanning electron microscope (SEM) with an accelerating voltage of 20 kV (JEOL Inc., Peabody, MA) at a magnification of 100×. The fractured surface of the tested specimens was sputter-coated with gold prior to SEM examination to avoid specimen charging.

Thermal Stability. Thermal stability is an important factor in bio-based nanocomposites as melt processing requires elevated temperatures. Inherently, bio-based nanocomposites suffer from low thermal stability which limits their application.[29] The thermal decomposition properties of pure PLA and nanocomposites were studied using thermogravimetric analyzer (TGA Q500, TA Instruments, New Castle, DE) over a temperature range 25–600 °C and a heating rate of 10 °C/min. The initial thermal decomposition temperature (T_{onset}), the maximum decomposition temperature (T_{peak}) and the final degradation temperatures (T_{endset}) were recorded.

Dynamic Mechanical Analysis. The viscoelastic properties of PLA and nanocomposites were studied using dynamic mechanical analyzer (DMA Q800, TA Instruments, New Castle, DE) following ASTM D4065. The bending method was used with a frequency of 1 Hz. The temperature was swept at a heating rate of 1 °C/min from 25 to 90 °C and the dynamic storage modulus (E'), loss modulus (E''), and the tan δ ($= E''/E'$) of each sample as a function of temperature were determined. Four replicates of each formulation were used in the DMA test.

Mechanical Property. The mechanical properties of PLA and nanocomposites are governed by microstructural parameters of matrix and nanofillers, the distribution of nanofiller in the matrix, and interfacial bonding between nanofillers and matrix.[30] Mechanical characteristics of PLA and nanocomposites were studied through tensile and impact tests. The tensile test was carried out using an Instron universal testing machine (Model 5567, Norwood, MA) following the ASTM D638 standard. Instron machine was equipped with a 30 KN load cell and the crosshead speed was set at 5 mm/min. An Izod impact tester (Tinius Olsen, Model Impact 104, PA) was used to run the impact tests and to calculate the impact strength of unnotched specimens following ASTM D256 standard.

Statistical Analysis

The mechanical properties data were statistically analyzed using one-way ANOVA and Tukey's tests. All statistical analyses were performed with a significance level of 5%. The data were analyzed by Minitab software version 17 (Minitab Inc., State College, PA). Eight replicates were used for each test.

RESULTS AND DISCUSSION

Morphology and Dimensions

The morphology of CNCs plays a critical role in nanocomposite properties and it is very important to ensure that the morphology of b-CNCs is not affected as a result of the surface modification. The morphological features of the modified and pristine CNCs after the dispersion in water were investigated using TEM images (Figure 2).

It was observed that modified CNCs maintained their elongated morphology with the mean values in the range 150–200 nm in length and 10–12 nm in width. The b-CNCs are thicker than CNCs and the results showed a reduction of 6.6–15.5% in the aspect ratio of b-CNCs.

Fractured Surface Morphology

The presence of CNCs aggregates and fracture pattern of nanocomposites were inspected through SEM images (Figure 3).

The smooth fractured surface of pure PLA exhibited some distinct river markings confirming the brittle character of PLA. The observed clean and smooth impact fractured surface in nanocomposites with low content of pristine CNCs (1 and 3 wt %) indicated the inherent stiffness and brittle fracture pattern in PLA-

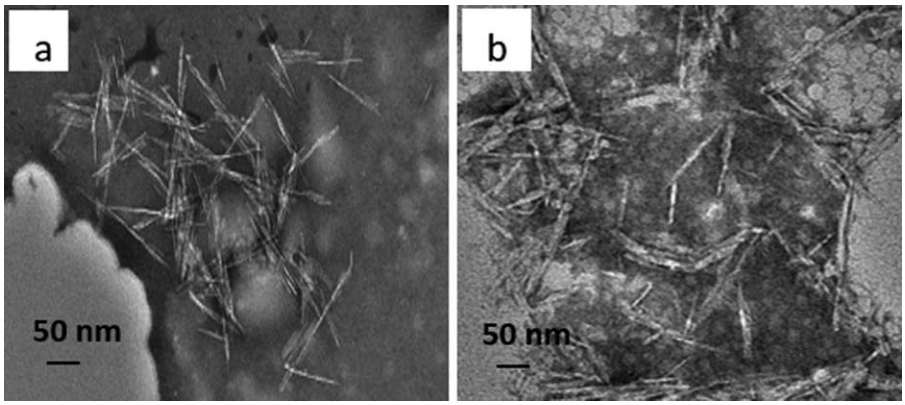

Figure 2. TEM images of (a) pristine CNCs and (b) modified CNCs.

1CNCs and PLA-3CNCs. However, nanocomposites with 1 and 3 wt % b-CNCs exhibited rough and irregular surfaces, suggesting the ductile fracture mechanism in PLA-1b-CNCs and PLA-3b-CNCs nanocomposites. In general, the fractured surface can illustrate the impact resistance of the materials.[31–33] The rough and irregular fractured surface in PLA-b-CNCs nanocomposites indicated more required work for impact fracture as compared with PLA-CNCs nanocomposites. It also suggested the higher impact resistance in PLA-b-CNCs nanocomposites than PLA-CNCs nanocomposites. Spherical voids, and cavities around visible CNCs aggregates mostly were observed in PLA-1CNCs, as shown in Figure 3(c). This behavior was an evidence of the interfacial debonding between PLA and CNCs owing to poor interfacial adhesion in PLA-CNCs nanocomposites.[34]

Thermal Stability

The influence of incorporating CNCs and b-CNCs into PLA on thermal stability of nanocomposite was investigated through TGA and derivative thermogravimetry (DTG) curves (Figure 4).

Thermal degradation through a one-step process was observed for pure PLA, PLA-1CNCs, and PLA-b-CNCs nanocomposites, indicating simultaneous degradation for all components. However, two distinct peaks were observed in PLA-3CNCs and PLA-5CNCs. This behavior can be attributed to the CNCs' isolation technique. The CNCs which used in this study were isolated from cellulose by a controlled hydrolysis using sulfuric acid (H_2SO_4).

The presence of two endothermic peaks confirmed that the sulfuric acid hydrolysis impacted the thermal stability of unmodified CNCs.[35]The first peak observed between 250 and 300 °C was small and the second peak which dominated the overall process occurred between 290 and 350 °C. The first peak was related decomposition of the negatively charged sulfate groups on CNCs and the second peak can be related to depolymerization of cellulose in competition with dehydration. These observations are corroborated by another study on cellulose nanomaterials treated with sulfuric acid.[27,36,37] Table II presents thermal characteristics of PLA and nanocomposites obtained from TGA and DTG curves.

The results on thermal properties of nanocomposites showed that PLA-b-CNCs nanocomposites were more thermally stable as compared with pure PLA, however, no significant change was observed with increasing b-CNCs content. The observed

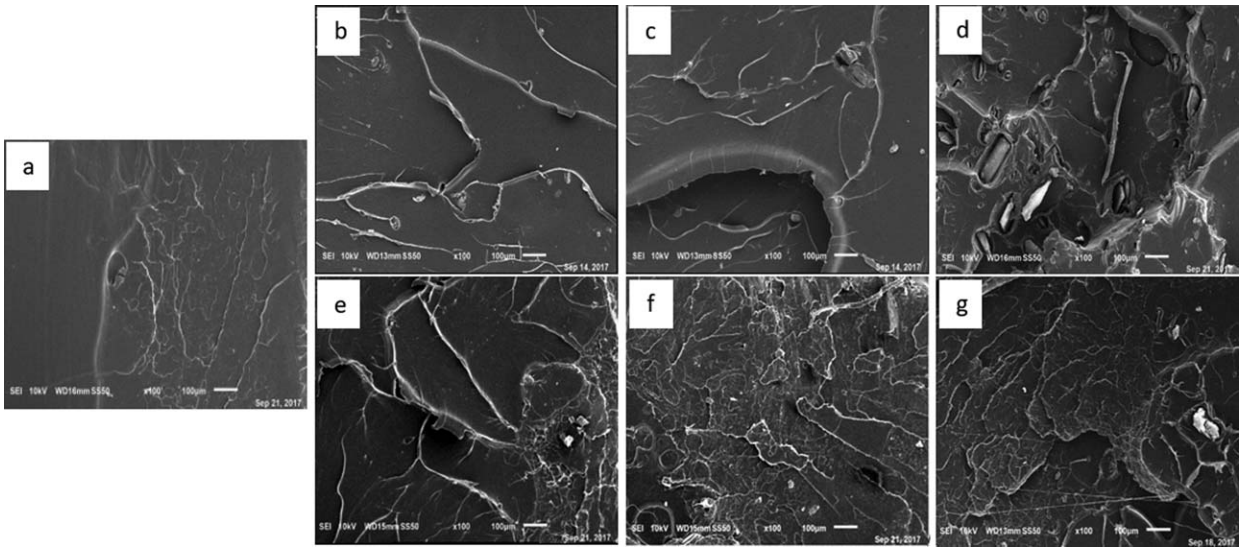

Figure 3. SEM images of fractured surface of (a) pure PLA, (b) PLA-1CNCs, (c) PLA-3CNCs, (d) PLA-5CNCs, (e) PLA-1b-CNCs, (f) PLA-3b-CNCs, and (g) PLA-5b-CNCs.

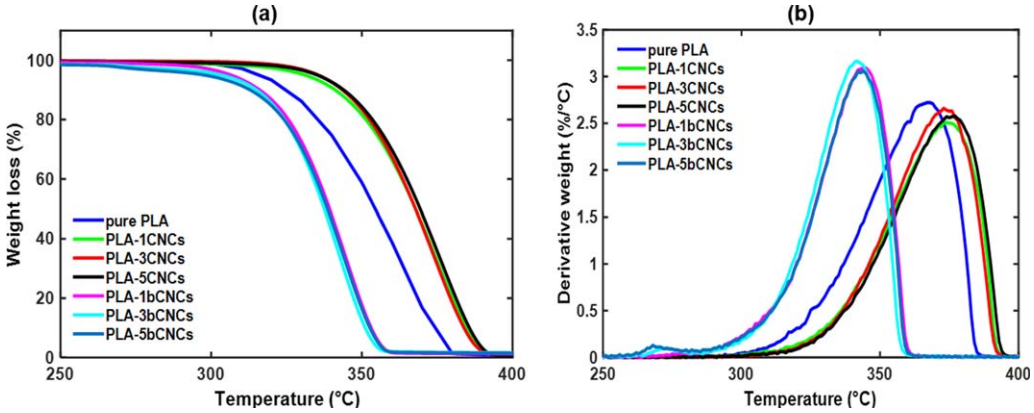

Figure 4. Representative (a) TGA and (b) DTG curves of PLA and nanocomposites. [Color figure can be viewed at wileyonlinelibrary.com]

improvement in thermal stability of PLA-b-CNCs nanocomposites was likely due to the increased dispersion of b-CNCs and the formation of stable hydrogen bonded networks between PLA and b-CNCs which hindered the degradation process of PLA-b-CNCs nanocomposites components.[23,38] PLA-CNCs nanocomposites exhibited an approximate decrease of 10% in thermal stability as compared with pure PLA. The application of sulfuric acid in CNCs isolation led to a lower temperature of thermal degradation for unmodified CNCs. It has been reported that treating cellulose with sulfuric acid can result in a reduction in thermal stability of CNCs, and an increase in char formation at the end of degradation process.[39,40]

DMA

The interaction between polymer molecular chains and organic nanoparticles as they are subjected to periodic loading under a range of temperatures can be illustrated using DMA. Figure 5(a) illustrates the effect of CNCs and b-CNCs concentrations on storage modulus at elevated temperatures. It was observed that the storage modulus of nanocomposites steadily increased with the incorporation of CNCs and b-CNCs as compared with pure PLA, which indicates the reinforcing effect of organic nanoparticles.[41] In particular, the storage modulus of PLA-b-CNCs nanocomposites was higher as compared with PLA-CNCs nanocomposites in the glassy state. This behavior was more likely due to the enhanced interfacial bonding between PLA and b-CNCs which resulted in better stress transfer from PLA matrix to b-CNCs. The maximum improvement in storage modulus was observed in PLA-3b-CNCs, however, with further increase in b-CNCs concentration to 5 wt %, storage moduli reduced owing to poor dispersion and agglomeration formation of b-CNCs in PLA matrix [Figure 3(f)].

Table II. Thermal Properties of PLA and Nanocomposites

Sample code	T_{onset} (°C)	T_{peak} (°C)	T_{endset} (°C)	Weight loss (%)
PLA	291.21	370.10	391.34	99.75
PLA-1CNCs	285.48	344.27	361.27	99.44
PLA-3CNCs	283.27	342.01	359.95	99.12
PLA-5CNCs	286.28	344.58	360.14	99.00
PLA-1b-CNCs	308.87	375.21	394.87	99.46
PLA-3b-CNCs	310.37	373.44	393.16	99.11
PLA-5b-CNCs	311.29	375.68	395.08	99.31

The tan δ curves as a function of temperature for PLA and nanocomposites are shown in Figure 5(b). The value of tan δ peak is an indication of viscoelastic behavior in nanocomposite and gives some information on the mobility of chain segments. The higher tan δ peak value typically means more energy dissipation potential in materials.[42]

The tan δ peak value of nanocomposites reinforced with b-CNCs exhibited lower values probably due to less viscous and more elastic behavior in PLA-b-CNCs nanocomposites as compared with PLA-CNCs nanocomposites. These results revealed better interfacial bonding between PLA matrix and b-CNCs.

The tan δ peak value, glass transition temperature (T_g), and storage modules in the glassy and rubbery states (below and above the T_g of samples) are summarized in Table III. The temperature at the peak value of tan δ curve is assigned as glass transition temperature (T_g) of the material.

Glass transition temperature is a complex property in the amorphous region of polymers and is governed by several factors such as chain flexibility and intermolecular interactions. DMA results show that the addition of CNCs or b-CNCs into PLA matrix does not noticeably affect the glass transition temperature of nanocomposites. The results implied that the interaction between PLA and cellulose nanocrystals slightly restricted the molecular mobility of the chains in polymer.[43]

Mechanical Property

The mechanical behavior of PLA and nanocomposites were evaluated through tensile and impact tests and the results are presented in Table IV. It was observed that the addition of b-CNCs had a stiffening effect on PLA matrix and improved Young's modulus, most likely due to the uniform dispersion of b-CNCs and improved interfacial adhesion between b-CNCs and PLA matrix. Similarly, an increase in the ultimate tensile strength was observed in PLA-b-CNCs nanocomposites in comparison with PLA-CNC nanocomposites with the same CNCs content. These results were in a good agreement with the SEM

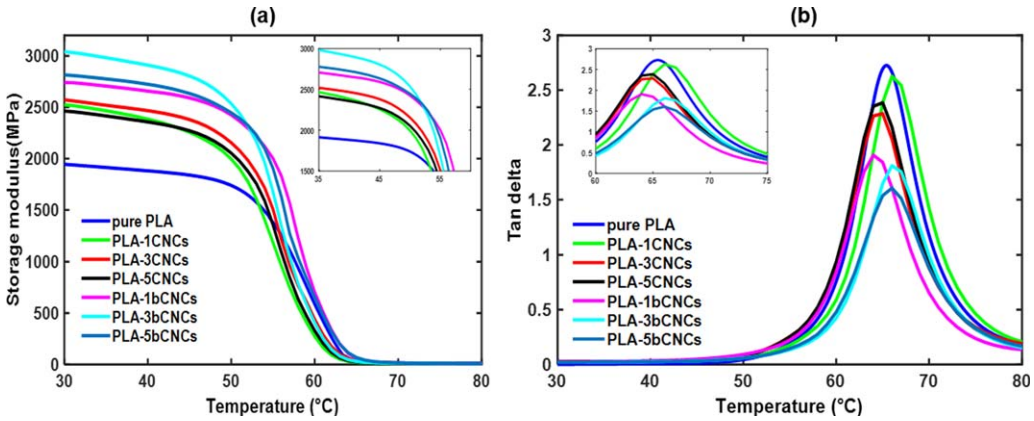

Figure 5. Representative (a) storage modulus and (b) tan δ versus temperature curves of PLA and nanocomposites. [Color figure can be viewed at wileyonlinelibrary.com]

Table III. Dynamic Mechanical Properties of PLA and Nanocomposites Obtained from DMA

			Storage modulus (MPa)	
Sample	T_g (°C)	Peak tan δ	30 °C	70 °C
PLA	64.05	2.72	1944 ± 56.7^{e}	15.62 ± 0.44a
PLA-1CNCs	66.77	2.62	2524 ± 12.17^{d}	8.69 ± 0.03^{c}
PLA-3CNCs	65.12	2.15	2708 ± 14.53^{c}	15.99 ± 0.48^{a}
PLA-5CNCs	65.48	2.38	2463 ± 14.11^{d}	9.29 ± 0.12^{c}
PLA-1b-CNCs	64.23	1.90	2740 ± 28.21^{bc}	11.54 ± 0.12^{b}
PLA-3b-CNCs	66.29	1.81	3041 ± 32.00^{a}	11.48 ± 0.09^{b}
PLA-5b-CNCs	66.58	1.60	2815 ± 24.60^{b}	15.72 ± 0.14^{a}

Different letters indicate a significant difference in the sample mean at $\alpha = 0.05$.

observations which showed more micro-size CNCs aggregates in PLA-CNCs nanocomposites compared with PLA-b-CNCs nanocomposites.

No significant differences were observed in elongation at break for nanocomposites reinforced with b-CNCs as compared with pure PLA, however, lower elongation at break was observed for PLA-CNCs nanocomposites. The observed reduction in the elongation at break for PLA-CNCs can be attributed to the weak interaction between PLA and CNCs. In the other words, the formation of relatively big CNCs aggregates in PLA-CNCs as shown in Figure 3, confirmed the weak interaction between PLA and CNCs and resulted in lower elongation at break. Higher values of impact strength were observed for all nanocomposite samples as compared with neat PLA which was more pronounced in the case of PLA-b-CNCs nanocomposites. Higher impact strength in PLA-b-CNCs can be attributed to the better interfacial interaction between PLA and b-CNCs and higher absorption of energy during impact test as compared with PLA-CNCs. This behavior was supported by a rough and irregular fractured surface in PLA-b-CNCs nanocomposites

Table IV. Mechanical Properties of PLA and Nanocomposites

Sample code	Young's modulus (GPa)	Ultimate strength (MPa)	Elongation at break (%)	Impact strength (kJ m^{-2})
PLA	$3.33 \pm 0.04^{f*}$	57.39 ± 1.20^{bc}	3.5 ± 0.14^{a}	20.90 ± 0.63^{c}
PLA-1CNCs	3.29 ± 0.19^{f}	52.76 ± 4.56^{d}	2.82 ± 0.51^{bc}	21.15 ± 2.01^{c}
PLA-3CNCs	3.37 ± 0.29^{df}	55.36 ± 4.21^{cd}	2.23 ± 0.31^{c}	21.22 ± 1.48^{c}
PLA-5CNCs	3.46 ± 0.30^{d}	55.57 ± 3.12^{cd}	2.47 ± 0.35^{c}	22.95 ± 0.25^{c}
PLA-1b-CNCs	4.74 ± 0.32^{c}	59.91 ± 2.18^{bc}	3.64 ± 0.25^{a}	24.15 ± 1.93^{b}
PLA-3b-CNCs	4.23 ± 0.39^{a}	63.66 ± 2.89^{e}	3.53 ± 0.35^{ab}	27.37 ± 2.35^{ab}
PLA-5b-CNCs	4.17 ± 0.16^{ab}	61.58 ± 2.01^{f}	3.65 ± 0.23^{a}	27.75 ± 1.39^{a}

Different letters indicate a significant difference in the sample mean at $\alpha = 0.05$.

observed from SEM images (Figure 3). Similar results were reported by Gao and Qiang[32] who showed higher impact strength for PLA-based nanocomposites with a rougher fractured surface.

CONCLUSIONS

The study compared the dispersion of pristine CNCs and esterified (b-CNCs) as a reinforcement in PLA matrix. Modified CNCs were prepared using a nontoxic and recyclable material through a solvent free and catalyzer free esterification technique. Nanocomposites were prepared by twin screw extrusion followed by injection-molding using masterbatch approach. Morphological properties of b-CNCs after esterification were studied using TEM images and no significant difference in the structure and shape of b-CNCs was observed as compared with unmodified CNCs. The fractured surface of PLA-b-CNCs showed increased surface roughness and contained fewer micro-size cellulose nanocrystal aggregates. These observations were further confirmed by the higher impact strength in PLA-b-CNCs nanocomposites as compared with PLA-CNCs. Higher thermal stability in PLA-b-CNCs nanocomposites was observed and can be attributed to of the esterification of CNCs which resulted in making b-CNCs more thermally stable. Although, a small reduction in the aspect ratio of b-CNCs was observed, higher mechanical properties in PLA-b-CNCs confirmed the treatment effect was more pronounced than the effect of aspect ratio of CNCs. The incorporation of b-CNCs improved the Young's modulus and ultimate tensile stress in PLA-b-CNC nanocomposites by 27.02 and 10.9%, respectively, however, the incorporation of pristine CNCs into PLA did not result in any significant change in the mechanical properties on PLA-CNC nanocomposites.

ACKNOWLEDGMENTS

The authors are grateful for the financial support from National Science Foundation, ND EPSCoR (grant no.11A1355466).

REFERENCES

1. Jonoobi, M.; Harun, J.; Mathew, A. P.; Oksman, K. *Compos. Sci. Technol.* **2010**, *70*, 1742.
2. Lim, L.-T.; Auras, R.; Rubino, M. *Prog. Polym. Sci.* **2008**, *33*, 820.
3. López de Dicastillo, C.; Garrido, L.; Alvarado, N.; Romero, J.; Palma, J. L.; Galotto, M. J. *Nanomaterials* **2017**, *7*, 106.
4. Masutani, K.; Kimura, Y. *Roy. Soc. Chem.* **2014**, *1*, 1.
5. Domenek, S.; Ducruet, V. Biodegradable and Biobased Polymers for Environmental and Biomedical Applications; John Wiley & Sons: Hoboken, New Jersey; **2016**, p 171.
6. Gupta, A.; Simmons, W.; Schueneman, G. T.; Hylton, D.; Mintz, E. A. *ACS Sustain. Chem. Eng.* **2017**, *5*, 1711.
7. Li, H.; Huneault, M. A. *Polymer* **2007**, *48*, 6855.
8. Al-Itry, R.; Lamnawar, K.; Maazouz, A. *Polym. Degrad. Stabil.* **2012**, *97*, 1898.
9. Bhardwaj, R.; Mohanty, A. K. *Biomacromolecules* **2007**, *8*, 2476.
10. Abdulkhani, A.; Hosseinzadeh, J.; Ashori, A.; Dadashi, S.; Takzare, Z. *Polym. Test.* **2014**, *35*, 73.
11. Gwon, J.-G.; Cho, H.-J.; Chun, S.-J.; Lee, S.; Wu, Q.; Li, M.-C.; Lee, S.-Y. *RSC Advances.* **2016**, *6*, 73879.
12. Valentini, L.; Cardinali, M.; Fortunati, E.; Torre, L.; Kenny, J. *Mater. Lett.* **2013**, *105*, 4.
13. Habibi, Y.; Lucia, L. A.; Rojas, O. J. *Chem. Rev.* **2010**, *110*, 3479.
14. Mariano, M.; Pilate, F.; de Oliveira, F. l B.; Khelifa, F.; Dubois, P.; Raquez, J.-M.; Dufresne, A. *ACS Omega* **2017**, *2*, 2678.
15. Yang, J.; Han, C.-R.; Zhang, X.-M.; Xu, F.; Sun, R.-C. *Macromolecules* **2014**, *47*, 4077.
16. Šupová, M.; Martynková, G. S.; Barabaszová, K. *Sci. Adv. Mater.* **2011**, *3*, 1.
17. Zhou, C.; Qiu, X.; Zhuang, Q.; Han, Z.; Wu, Q. *J. Appl. Polym. Sci.* **2012**, *124*, 4740.
18. Prathapan, R.; Berry, J. D.; Fery, A.; Garnier, G.; Tabor, R. F. *ACS Appl. Mater. Interfaces* **2017**, *9*, 15202.
19. Ng, H.-M.; Sin, L. T.; Tee, T.-T.; Bee, S.-T.; Hui, D.; Low, C.-Y.; Rahmat, A. *Compos. Part B: Eng.* **2015**, *75*, 176.
20. Bagheriasl, D.; Carreau, P. J.; Riedl, B.; Dubois, C.; Hamad, W. Y. *Cellulose* **2016**, *23*, 1885.
21. Goussé, C.; Chanzy, H.; Excoffier, G.; Soubeyrand, L.; Fleury, E. *Polymer* **2002**, *43*, 2645.
22. Yuan, H.; Nishiyama, Y.; Wada, M.; Kuga, S. *Biomacromolecules* **2006**, *7*, 696.
23. Spinella, S.; Re, G. L.; Liu, B.; Dorgan, J.; Habibi, Y.; Leclere, P.; Raquez, J.-M.; Dubois, P.; Gross, R. A. *Polymer* **2015**, *65*, 9.
24. Yoo, Y.; Youngblood, J. P. *ACS Sustain. Chem. Eng.* **2016**, *4*, 3927.
25. Herrera, N.; Mathew, A. P.; Oksman, K. *Compos. Sci. Technol.* **2015**, *106*, 149.
26. Roggio, G. AMASE Master Program. Department of Engineering Sciences and Mathematics Luleå University of Technology; **2014**, Luleå, Sweden.
27. Gazzotti, S.; Farina, H.; Lesma, G.; Rampazzo, R.; Piergiovanni, L.; Ortenzi, M. A.; Silvani, A. *Eur. Polym. J.* **2017**, *94*, 173.
28. Espino-Pérez, E.; Domenek, S.; Belgacem, N.; Sillard, C.; Bras, J. *Biomacromolecules* **2014**, *15*, 4551.
29. de Castro, D. O.; Bras, J.; Gandini, A.; Belgacem, N. *Carbohydr. Polym.* **2016**, *137*, 1.
30. Gojny, F. H.; Wichmann, M. H.; Fiedler, B.; Schulte, K. *Compos. Sci. Technol.* **2005**, *65*, 2300.
31. Mandelbrot, B. B.; Passoja, D. E.; Paullay, A. J. *Nature* **1984**, *308*, 721.
32. Gao, H.; Qiang, T. *Materials* **2017**, *10*, 624.
33. Okubo, K.; Fujii, T.; Thostenson, E. T. *Compos. Part A: Appl. Sci. Manuf.* **2009**, *40*, 469.
34. Xu, X.; Liu, F.; Jiang, L.; Zhu, J.; Haagenson, D.; Wiesenborn, D. P. *ACS Appl. Mater. Interfaces* **2013**, *5*, 2999.
35. Gong, J.; Li, J.; Xu, J.; Xiang, Z.; Mo, L. *RSC Adv.* **2017**, *7*, 33486.

36. Yildirim, N.; Shaler, S. *Materials* **2017**, *10*, 718.
37. Parit, M. Master Degree Thesis, Auburn University **2016**.
38. Dhar, P.; Tarafder, D.; Kumar, A.; Katiyar, V. *RSC Adv.* **2015**, *5*, 60426.
39. Chen, Y. W.; Tan, T. H.; Lee, H. V.; Abd Hamid, S. B. *Materials* **2017**, *10*, 42.
40. Chen, L.; Zhu, J.; Baez, C.; Kitin, P.; Elder, T. *Green Chem.* **2016**, *18*, 3835.
41. Grunert, M.; Winter, W. T. *J. Polym. Environ.* **2002**, *10*, 27.
42. Hill, D.; Perera, M.; Pomery, P.; Toh, H. *Polymer* **2000**, *41*, 9131.
43. Yamanobe, T.; Ueki, K.; Komoto, T.; Uehara, H. *Polym. J.* **2012**, *44*, 764.